Preparation of Nanocellulose from Kenaf (*Hibiscus cannabinus L.*) via Chemical and Chemo-mechanical Processes

8

Paridah Md. Tahir, Lukmanul Hakim Zaini, Mehdi Jonoobi, and H. P. S. Abdul Khalil

Contents

Keywords

Kenaf • Kenaf cellulose whiskers • Nanocellulose • Chemo-mechanical

---

P.M. Tahir (✉) • L.H. Zaini
Biocomposite Technology Laboratory, Institute of Tropical Forestry and Forest Products, Universiti Putra Malaysia (UPM), Serdang, Selangor, Malaysia
e-mail: parida.introp@gmail.com; lukmanulhakimzaini@yahoo.com

M. Jonoobi
Department of Engineering Sciences and Mathematics, Lulea University of Technology, Lulea, Sweden
e-mail: mehdij1978@gmail.com

H.P.S. Abdul Khalil
School of Industrial Technology, Universiti Sains Malaysia, Penang, Malaysia
e-mail: akhalilhps@gmail.com

1   Introduction

A fundamental understanding of the relationships between basic fiber properties, methods of processing, and composite end use performance properties has been well developed due to recent advances within the biocomposites research community. Simultaneously, advanced engineered biocomposites are currently being developed to meet the diverse needs of users for high-performance materials as well as economical commodity products. Advancements in nanotechnology have led to industrial isolation of nanocrystalline cellulose [1, 2]. While nanocrystalline cellulose may be only 1/10 as strong as carbon nanotubes – currently the strongest known structural material [3, 4] – it may cost 50–1,000 times less to produce [5, 6]. Engineered biocomposites employing nanocrystalline cellulose reinforcement could soon provide advanced performance, durability, value, service life, and utility, while at the same time being a fully sustainable technology.

A critical tool to achieve the goal of developing advanced biocomposites requires using the new science of nanotechnology to manipulate and control materials and processes at the nanoscale. Once many of its apparent promises are achieved, nanotechnology may well present a major tool to improve structural performance and extend serviceability by orders of magnitude. The next generation of engineered biocomposites needs to provide materials and products that far exceed current expectations. Whether it is for construction, building, automotive, marine, or aerospace, such products need to be of lower cost, higher performance, and lower maintenance and more adaptable and reliable and possess smart material properties.

Some characteristics of these products are [7]:

1. Able to develop synergistic performance through combination of wood, inorganic materials, and natural biofiber
2. Provide enhanced performance and superior serviceability
3. Be more durable, dimensionally stable, moisture proof, and fire resistant
4. Possess advanced sensory capabilities for warning users when problems are imminent
5. Possess advanced biomimetic capabilities for fixing itself when problems are encountered
6. Be renewable, recyclable, and sustainable
7. Decrease environmental impacts from processing and use
8. Have both materials and processes engineered to customize and optimize performance

According to Winandy et al. [7], nanotechnology offers three potential opportunities for the development of advanced lignocellulosic-based biocomposites:

1. Development of new analytical technologies that will provide a fundamental understanding of material behavior at the nanoscale.
2. Application of nanoparticles (inorganic and organic) in advanced biocomposites to enhance its performance.
3. Modifications of the wood and lignocellulosic raw material surfaces at the nanoscale.

This knowledge will then provide tools with which we can begin to fundamentally understand and then possibly control and manipulate critical materials–process–performance relationships.

1.1   Nanocellulose

Even though nanocellulose was introduced in the 1970s by Turbak, Snyder, and Sandberg in New Jersey, USA, it is not until the mid-1990s that it was taken up by the Japanese group, first by Taniguchi and co-workers and later by Yano and co-workers [8]. In the USA, a host of major companies such as P&G©, J&J, 3 M©, McNeil, etc. have used this technology in their products. Today, there are still extensive research and development efforts around the world in this field.

Nanocellulose or sometimes known as microfibrillated cellulose (MFC) can be prepared from any cellulose source material, but wood pulp is normally used. The nanocellulose fibrils are isolated from the wood-based fibers using high-pressure homogenizers which are controlled by speed, temperature, and pressure. The homogenizers are used to delaminate the cell walls of the fibers and liberating the nano-sized fibrils. This production route is normally connected to high energy consumptions (usually over 30 MWh/ton) being associated with the fiber delamination. Pretreatments such as enzymatic/mechanical and introduction of charged groups, e.g., through carboxymethylation or TEMPO-mediated oxidation [9], are sometimes used to address this problem. Another type of nanocellulose is cellulose nanowhiskers, a more crystalline form of nanocellulose which is formed by acid hydrolysis of native cellulose fibers using a concentrated inorganic salt, commonly sulfuric or hydrochloric acid. The amorphous sections of native cellulose are hydrolyzed, and after careful timing, the crystalline sections can be retrieved from the acid solution by centrifugation and washing. Cellulose nanowhiskers are rod-like highly crystalline particles (relative crystallinity index above 75 %) with a rectangular cross section. Its dimensions depend on the native cellulose source material, and hydrolysis time and temperature. Nanowhiskers are shorter (100–1,000 nm) than the nanofibrils obtained through the homogenization route (10 nm to several microns).

Nanocellulose/MFC is composed of nano-sized cellulose fibrils with a high aspect ratio (length to width ratio). Typical lateral dimensions are 5–20 nm, and the longitudinal dimension is in a wide range from 10s of nanometers to several microns. Nanocellulose is a pseudoplastic and exhibits the property of certain gels or fluids that are thick (viscous) under normal conditions, but flow (become thin, less viscous) over time when shaken, agitated, or otherwise stressed. This property is known as thixotropy. When the shearing forces are removed, the gel regains much of its original state.

The unique rheology of nanocellulose dispersions was recognized by the early investigators [10]. The high viscosity at low nanocellulose concentrations makes

nanocellulose very interesting as a non-calorie stabilizer and gellant in food applications, the major field explored by the early investigators. The dynamic rheological properties have been investigated in great detail [11], and it has been found that the storage and loss modulus were independent of the angular frequency at all nanocellulose concentrations between 0.125 % and 5.9 %. The storage modulus values are particularly high (104 Pa at 3 % concentration) compared to results for cellulose nanowhiskers (102 Pa at 3 % concentration). There is also a particular strong concentration dependence as the storage modulus increases 5 orders of magnitude if the concentration is increased from 0.125 % to 5.9 %.

It has long been known that crystalline cellulose has interesting mechanical properties for use in material applications. The stiffness of crystalline cellulose has been shown to be in the order of 140–220 GPa, which is comparable to Kevlar and is better than glass fibers that are currently used as reinforcement for plastics. Films made from nanocellulose have been shown to have high strength (over 200 MPa), high stiffness (around 20 GPa), and high strain (12 %).

1.2   Kenaf

Agro-based lignocellulosics intended for use in composite products can be categorized into two types: agricultural residues and lignocellulosics grown specifically for their fiber. The residue types include sugarcane bagasse, cereal straws, coconut coir, corn stover, oil palm stems and empty fruit bunch, and cotton stalks, whereas planted crops are annual crops that originate from various sources such as hemp, flax, sisal, abaca, jute, ramie, kenaf, etc.

> The overall limitations for using agricultural lignocellulosic materials include: lack of established delivery systems, processing complications caused by fiber density and morphology, process-temperature limitations, risk of decay, and or emission during processing and use [62].

Low thermal-degrade temperatures, high volatile emissions, and high moisture absorption of agro-fibers may also limit their processing options [68]. Compared to wood fiber, agro-fibers have lower density, higher stiffness-to weight ratio, and enhanced recyclability and biodegradability [62]. Although inorganic fibers such as fiberglass are stronger, bio-fibers have a more desirable balance of strength to weight.

Kenaf is categorized as hard fiber plant that comprises woody inner core and fibrous outer bast which provide excellent source of cellulose fibers. The proportion of these two sections is different based on stem height that normally contains about 35 % bast and 65 % core. Separation of long fibers from the bast generates higher monetary returns over whole stalk kenaf. The quality of the resulting fibers, however, depends on several factors among others which include methods of separation, machinery involved, chemical used, and state of the stem prior to separation [12].

1.2.1 History of Kenaf

There are many factors that make kenaf more attractive than the other bast fibers such as hemp, flax, and jute. Kenaf is a warm-season annual fiber crop growing in temperate and tropical areas. The height of this plant can reach 2.7–3.6 m, and the fiber, the most valuable part, can be extracted from its bark or bast. The characteristics of kenaf fibers are similar to those of wood, and the yields of kenaf are greater than those of hemp, flax, and jute, thus providing more cost-effective raw materials [13–15]. The fiber from kenaf is usually used to manufacture products such as grade pulps for the pulp and paper industry, protective packaging for fruits and vegetables, filters, composite boards, and textile.

The interest in kenaf started way back in the 1960s where the United State Department of Agriculture (USDA) has embarked on a large screening of potential plant crops for fiber production [16]. Kenaf has been listed together with other fiber crops such as jute, hemp, flax, and ramie. Japan has been the world major consumer of wood-fiber papers is keen on increasing its usage of non-wood fiber and is reported to have indicated its preference for kenaf as the preferred feedstock. India, China, and Thailand account for 90 % of world plantation with more than 95 % of world production of kenaf. In 2005–2006, total kenaf production was 0.33 million tons of which India, China and Thailand produced 42 %, 25 % and 11 %, respectively, while other countries produced the difference [17].

Compared to wood, kenaf production yields are favorable. Kenaf fiber can achieve an average of 17.8 metric tons (t) per hectare (ha) per annum (a) versus 2.2 ton/ha for tree fiber. Therefore, a significant contribution to the supply of raw material for cellulose pulp and other product from kenaf plants potentially substitutes wood resources. Kenaf fibers have been considered as reinforcing agents in polymer matrix [18]. The cell walls of lignocellulosic fiber are formed from oriented reinforcing semicrystalline cellulose microfibrils embedded in a hemicellulose/lignin matrix of varying composition. These microfibrils are made of cellulose molecules in extended chain conformation which provide the strength to the fibers, with a typical diameter of about 30–100 nm [19]. At this size, the cellulosic microfibrils can actually be considered to be nanofibers.

1.2.2 Anatomical Structures of Kenaf Fibers

Generally, kenaf bast fiber bundles are composed of elongated thick-walled ultimate cells which are joined together, both end to end and side by side, forming aggregates of fiber bundles along the height of the tree stem. During growing period of the stem, a circumferential layer of primary fibers is developed from the protophloem, but as vertical growth ceases in the lower parts, the secondary phloem fibers (where the bast fibers can be obtained) are developed as a result of cambial activity. Figure 8.1 shows a cross section of cell structure of kenaf stem. Unlike cotton which is unicellular, kenaf fibers have multicellular type cells. Depending on the location in the stem, kenaf contains three types of fiber: bast, core, and pith. Bast fiber is long and has thick cell wall, while those of core fiber are thinner with much

Fig. 8.1 Cross section of kenaf stem: bark (*lower part*) and core (*upper part*) in transverse section
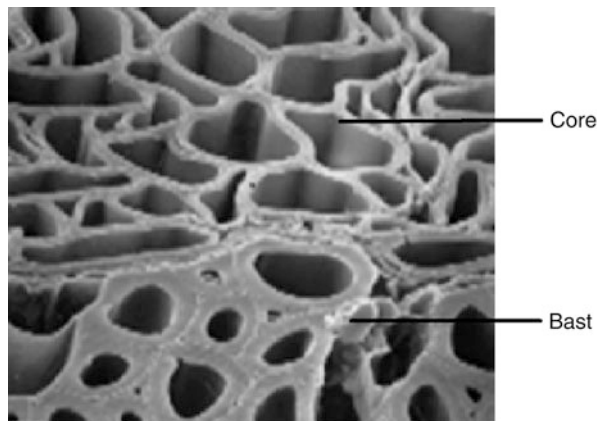
shorter fiber length [20]. The core fibers appear as wedge-shaped bundles of cells and intermingle with parenchyma cells and other soft tissue. The pith consists exclusively of parenchymatous cells which are not typically prismatic but polygonal in shape. During fiber processing, the pith particles dried up and naturally detached from the rest of the fibers. In mature plants, kenaf can reach a height of 2.5–3.5 m [21]. Zhang [22] reported that the lengths of kenaf fibers are shorter at the bottom of the stalk and longer at the top. The increase in fiber length from the bottom to the top was found not to be gradual, but S-shaped [23]. Fiber length grew in the early part of the plant cycle and reduced again as the plants mature [24]. Kenaf single fibers are only about 1–7 mm long and about 10–30 μm wide, thus too short for textile processing [25].

Several studies have reported the anatomical structure of kenaf stem [21, 23, 26, 27]. The core fibers have larger lumen and a thinner cell wall than bast fibers. The width of the bast fibers is lower than that of the core fibers. The average kenaf fiber length from three kenaf cultivars was 2.45 mm and the average fiber width was about 12 μm [28]. Fiber length and width were similar among those cultivars and also similar at different stages of maturity. The core has very similar proportion of chemicals content of wood, while bastfiber was different. Table 8.1 compares basic properties of kenaf fibers with other types of bast fibers [20]. Apparently, kenaf varies greatly in terms of chemical properties, tensile strength, and equilibrium moisture content (EMC). Such differences may be attributed to the retting method employed when extracting the long fibers.

Many studies have been conducted on isolated nanofibers from cellulosic materials such as hemp, wheat straw, and wood pulp using nano reinforcements in polymer matrix [37–39]. These studies have derived a common conclusion to use nanofibers in various polymer matrices as reinforcement to improve the mechanical properties of the resulting nanocomposites. Nanofibers derived from cellulose fibrils contain nano-sized microfibrils that have high structural strength and stiffness [38]. Because of this reason, cellulose nanofibers have gained the world attention since the last decade, mainly on extracting cellulose microfibrils from

Table 8.1 Characteristics of long bast fibers produced from hemp, jute, flax, and kenaf

| Type | Fiber length (mm) | Fiber diameter (microns) | Fiber chemical content | | | | Tensile strength (mm) | EMC (%) | Retting methods | References |
			Lignin (%)	Cellulose (%)	Pectin (%)	Hemicellulose (%)				
Hemp	15–55	17–22.8	5–3	70–92	0.9	18–22	310–750	<15	Chemical retting	5,7, 14,15,16,17,18
Jute	2–5	15.9–20.7	5–13	51–84	0.2	12–20	200–450	23	Dew retting	5,7,8,9
Flax	9–70	5–38	14–19	60–81	0.9	2.3	345–1,100	10–12	Enzymatic retting	2,5,7,9, 11,12
Kenaf	2.6–4	17–21.9	15–19	44–57	2	21	295–1,191	10–20	Water retting	1,2,3,4,5,6

Source: 1-Misra [29]; 2-Mohanty et al. [30]; 3-Rowell and Han [23]; 4-Anon [31]; 5-Calamari et al. [25]; 6-Chen et al. [24]; 7-Sikorski [32]; 8-Gassan et al. [66]; 9-Rowell and Stout [21]; 11-Alann [67]; 12-Biogiotti et al. [48]; 14-Kozlowski [15]; 15-Mwaikambo and Ansell [33]; 16-Preston [34]; 17-Ranalli [35]; 18-Mwaikambo [36]

various natural sources and using them as reinforcement in composite manufacturing [40, 41]. Nevertheless, since this is a relatively new field, the most challenging element would be in the extraction technique, i.e., fiber isolation and separation processes, which involve cleavage of the strong hydrogen bonding [42]. Thus, limitations on low yield, entanglement of fibers, and dispersion of fiber are anticipated that makes it uneconomical for pilot-scale production.

There are essentially many ways to extract cellulose nanofibers. This chapter discusses preparation of cellulose whiskers from kenaf via sulfuric acid reaction and extraction of nanofibril using chemo-mechanical processes.

2   Materials and Methods

2.1   Preparation of Cellulose Whiskers from Kenaf Bast Fibers

Four-month-old kenaf (*Hibiscus cannabinus* L.) from variety V36 was used to prepare the nanocellulose. Kenaf stems were peeled to separate the outer (bast) from the inner (core) part. Kenaf basts and core were dried to <10 % moisture content in an industrial oven. The dried bast fibers were kept in plastic bags and stored in dry condition until further use.

The process of whiskers production from kenaf bast was adopted from [63] with some modification in speed and time of centrifugation. The sequence of work is briefly illustrated in Fig. 8.2. Firstly, the kenaf bast was ground using a FRITSCH universal cutting mill pulverizer. The powdered bast was then treated with 4 % (w/w) NaOH solution at 80 °C for 2 h. At the end of reaction, the fibers were washed with distilled water and filtered. These steps (from alkali treatment to washing) were repeated three times until the alkali was completely removed. Subsequently, a bleaching treatment was applied by soaking the fiber in a solution containing equal parts of acetate buffer, aqueous chlorite 1.7 % (w/w), and distilled water. Then the fibers were washed with distilled water and filtered. The bleaching sequence was repeated four times under mechanical stirring.

Acid hydrolysis was performed by subjecting 4–6 % (w/w) kenaf bast bleached fibers in preheated sulfuric acid (65 %) at 50 °C for 60 min. The suspension was constantly mixed using magnetic stirrers. Separation was carried out in a centrifuge maintained at 4,000 rpm for 30 min and dialyzed with distilled water. Subsequently, whiskers suspension was homogenized by using an Ultra Tura T25 homogenizer for 5 min. Several drops of chloroform were added to the whiskers suspension to protect against bacteria growth. The whiskers suspension was stored at 4 °C.

2.2   Preparation of Kenaf Nanofibers Using Chemo-mechanical Process

The whole kenaf stem, bast, and core were used in this study. Kenaf bast was stripped from the core manually and immersed in water at 1:20 (bast to water) until
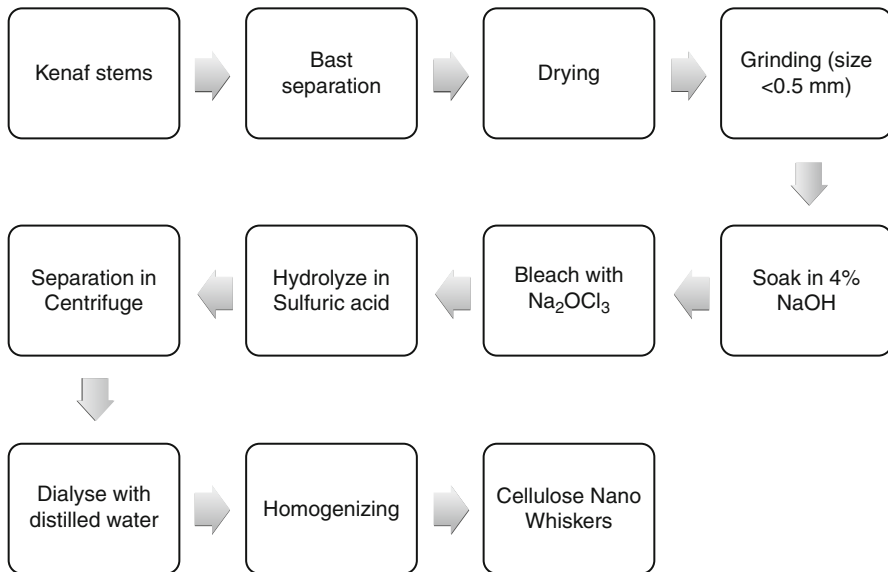
Fig. 8.2 Flow chart for preparing cellulose whiskers from kenaf bast

the fibers were loosened and separated out from the bast. The water-retted bast fibers were then air-dried prior to pulping.

2.2.1   Pulping and Bleaching

Kenaf bast fibers were cut to lengths of 2–3 cm, whereas kenaf whole stem and core were chipped into 2–3 cm dimension. Subsequently, 300 g of oven-dried, short kenaf fibers were cooked in a digester (MK model, USA) with NaOH 15 % and 0.1 % of anthraquinone (AQ). The ratio of cooking liquid to kenaf fibers was 7:1. The maximum cooking temperature was set to 160 °C, and this temperature was reached after 60 min. Another 45 min of cooking were carried out at the maximum temperature. Table 8.2 lists the conditions of the NaOH-AQ pulping process applied in this study. A three-stage bleaching was performed to ensure complete removal of hemicellulose and lignin. Table 8.3 shows the conditions of the bleaching processes.

2.2.2   Mechanical Treatments

Bleached and unbleached kenaf pulps (with dry weights of 24 g) were immersed in distilled water for 8 h. The fibers were distributed in the water using a laboratory disintegrator (Ihon-Rigoku-SP ¼ Japan model) at 3,000 rpm for 20 min. A pulp mat, which has a total weight of 240 g, was prepared with 10 % fiber concentration. With the purpose of defibrillating the fibers, the mat was then placed in a laboratory-type PFI mill (PTI Australian model) with a treatment level of 100,000 revolutions. Subsequently, the refined pulp was immersed in liquid nitrogen, where it was subjected to a cryo-crushing process, as developed by Bhatnagar and Sain [43]. According to this

Table 8.2 Condition of
NAOH-AQ pulping process

Cooking process	NaOH-AQ
NaoH (%)	15
Anthraquinone (AQ) (%)	0.1
Liquor to fiber ratio	7:1
Maximum temperature (°C)	160
Time to maximum temperature (min)	60
Time at maximum temperature (min)	45–75

Table 8.3 Conditions of bleaching process

Stage	D1	Ep	D2
Chemical charged	Sodium chlorite (2 %)	NaOH (1.5 %)	Sodium chlorite (1.25 %)
	Acetic acid (3 %)	H_2O_2 (1 %)	Acetic acid (3 %)
Pulp consistency	10 %	10 %	10 %
Temperature	70 °C	70 °C	70 °C
Time	180 min	90 min	90 min

method, the pulp was placed in liquid nitrogen and crushed using a mortar and pestle. Crushed pulp was then washed with distilled water and filtered.

Diluted suspensions (0.2 %) of bleached and unbleached pulp were prepared, and the nanofibers were individualized with a high-pressure homogenizer (APV-1000). Prior to the homogenization process, all suspensions were ground in a mechanical blender apparatus for 15 min. The suspensions were passed through the homogenizer 40 times, and the pressure was held constant at 500 bar.

2.3   Fiber Analysis and Characterization

2.3.1   Fiber Yield
A small amount of the sample from each treatment was oven-dried at 105 °C for 24 h. The dried specimen was kept in a desiccators prior to weighing. The yields after each stage of chemical treatment were calculated as percentage of dried fiber over initial weight of kenaf sample.

2.3.2   Morphology of Fibers
A Philips XL30 ESEM was used to study the effect of the treatments on the fiber morphology. The acceleration voltage was set to 20 kV; all samples had been sputter coated with gold to avoid charging. The structure and size of the nanofibers were studied by transmission electron microscopy on a Hitachi model H-7100. A drop of diluted kenaf nanofiber suspension was deposited on the

carbon-coated grid and allowed to dry at room temperature. Measurements of the fiber diameters were carried out using an image analyzer program, XL Docu. Totally, 150 fibers of each material were measured.

2.3.3   Chemical Analysis

The chemical compositions of kenaf fibers before and after chemical treatment were determined according to TAPPI standard, 203 om-93. The percentages of holocellulose and lignin were determined following Wise and Murphy [44] and TAPPI standards, 222 om-88, respectively.

2.3.4   Field Emission Scanning Electron Microscopy (FE-SEM)

Glimmer plates were fixed with conducting carbon on a specimen holder. A drop of diluted fibril/water suspension (1:20) was put onto it. The samples were air-dried and the remaining fibrils were sputtered with a platinum layer of about 5 nm. The images were taken with 2 kV accelerating voltage.

2.3.5   Transmission Electron Microscope (TEM) Characterization

The size and shape of whiskers were studied under a transmission electron microscope (TEM) Hitachi model H-7100. A drop of diluted kenaf whiskers/chemo-mechanical nanocellulose suspension that was prior stained with 0.5 % solution of uranyl acetate was deposited onto a carbon-coated grids plate and allowed to dry at room temperature.

The nanocomposite film sample was evaluated for nanostructure and whiskers/chemo-mechanical nanocellulose distribution by TEM at an acceleration voltage of 100 kV. A small rectangular sample was cut to 2×7 mm^2 in size from the film. The cut specimens were then embedded in a mix of Benzyldimethylamine (BDMA), methyl nadic anhydride (MNA), and dodecenyl succinic anhydride (DDSA) resins and cured for 2 days. The final ultra microtoming was performed with a diamond knife at room temperature generating electron transparent foils, being approximately 50 nm in thickness. The foils were gathered on 300 mesh Cu grid. The fiber's diameter measurements were carried out using an image analyzer program, XL Docu.

2.3.6   Fourier Transform Infrared Spectroscopy (FTIR)

The Fourier transform infrared spectroscopy (FTIR) study was done using Perkin-Elmer spectrometer 100, USA. Prior to this analysis, crude fibers, alkali-treated fibers, bleached fiber kenaf whiskers, and chemo-mechanical nanocellulose were prepared by grinding into 100 μm sized powder, mixed with KBr, and pressed into transparent pellets. In the case of thin nanocomposite film (containing cellulose acetate butyrate (CAB) and kenaf whiskers), the analysis was done within the range of 4,000–500 cm^{-1} transmittance mode.

2.3.7   X-Ray Diffraction

The structural and phase analysis of the samples was performed using the X-ray diffractometer (Philips P W 3040/60 X$^{|}$ pert Pro) with CuKα radiation (wavelength

of 1.5405 Å) and step-scan mode (2θ range: 5–50°). The phase identification of the samples was performed using the X' Pert Highscore software with the support of ICDD PDF-2 database, and the lattice parameter was calculated using the X' pert plus. The crystalline index of cellulose, C_{Ir}, was calculated using the following equation (Segal empirical method 1959):

$$C_{Ir}(\%) = [(I_{002} - I_{am})/I_{002}] \times 100$$

where I_{002} is the intensity of lattice peak diffraction and I_{am} is the peak intensity of the amorphous fraction. A diffraction angle of around 2θ = 22.5° was peak for plane (002), and the lowest intensity at a diffraction angle of around 2θ = 18.0° was measured as the amorphous part.

2.3.8   Thermogravimetric Analysis (TGA)

Thermal stability data was obtained using thermogravimetric analyzer (TGA Q500 – TA instruments) under linear temperature conditions. The samples (10.0 ± 1.0 mg) were heated in a platinum pan at 25–600 °C, with a heating rate of 10 °C/min in a nitrogen atmosphere.

3   Results and Discussion

3.1   Properties of Kenaf Cellulose Whiskers

Cellulose comprises between 35 % and 50 % of the total dry mass and consists of long chains of β-anhydroglucose units linked by β1,4-glucoside bonds. About 50–90 % of the cellulose in lignocellulosic materials is bound laterally by hydrogen bonds and forms crystalline structure. The remaining portion is less ordered and is often called amorphous cellulose [45]. It is the crystallinity of cellulose that poses the first of the major challenges in effective hydrolysis. Accessible surface area is another challenge for effective hydrolysis and this can be overcome by pretreating the fiber in NAOH prior to acid hydrolysis [33]. Another significant challenge in cellulose hydrolysis is the physical protection of cellulose provided by hemicellulose and lignin. Hence, in all the production of whiskers from woody materials, bleaching via oxidation of both hemicellulose and lignin is essential to ensure pure cellulose is produced for the next hydrolysis sequence. Reaction conditions vary from fiber types and origins.

3.1.1   Whiskers Yield

The yield of kenaf whiskers after each chemical treatment was calculated based on initial weight of kenaf fiber before treatment. The results show that 50 % of fibers can be collected upon NaOH treatment. Alkali treatment has apparently degraded almost all lignin and hemicellulose that normally present, respectively, between 15–19 % and 21 % (see Table 8.1). Subsequent bleaching further removed the remaining lignin, thus reducing the fiber yield to only 38 %. It was obvious that almost pure cellulose has been obtained as the color of the fibers was almost white

Fig. 8.3 Yields of kenaf fiber after alkali treatment (*A*), after alkali treatment and bleaching (*B*), and after alkali treatment, bleaching, and acid hydrolysis – cellulose whiskers (*C*)
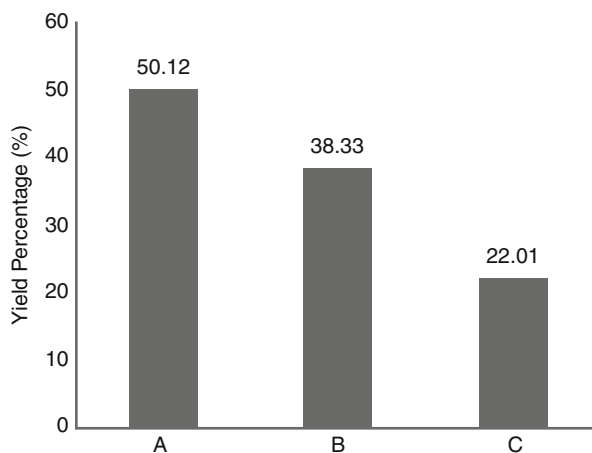

indicating all lignin has been extracted. Upon acid hydrolysis, this "cellulose" yielded about 22 % cellulose whiskers (Fig. 8.3).

3.1.2 Fiber Morphology

The isolation of whiskers from kenaf bast is a multistep processes which involve chemical treatments. Hence, optimum chemical treatments are needed to avoid damage on the cellulose. Figure 8.4a–c exhibits field emission scanning electron micrograph images of kenaf bast fiber after it has undergone three steps of fiber treatment: alkali, bleaching, and acid hydrolysis. There was noticeable reduction in size after more treatments were applied to the fibers. Figure 8.4a shows untreated (crude) kenaf bast single fiber having almost similar diameter size which is around 100 μm. After being treated with NaOH, the diameter of the fiber reduced to a wider range, 20–90 μm, due to unequal reaction with alkali Fig. 8.4b. On further reaction with aqueous chlorite (bleaching stage), sufficient energy appears to be formed that breaks the lignin in the middle lamella that bonds the fibers together. Consequently smoother surface individual fibers revealed as can be seen in Fig. 8.4c. At this point, diameter of the fibers reduced to an average 11 ± 3 μm.

Figure 8.4d shows whiskers with a needle-like structure. The tendency to agglomerate could also be observed from this image which is to be expected as the cellulose crystals loss its H-bonding when the water evaporates during drying. Figure 8.5 shows the diameter distribution of whiskers extracted by sulfuric acid hydrolysis. Based on measurements of 150 individual whiskers, the diameter of cellulose whiskers was between 2 and 5 nm; most of the samples had diameter within 2–4 nm. The average diameter of cellulose kenaf whiskers was 3.03 nm. Compared to whiskers extracted from sugarcane bagasse which was 4 ± 2 nm [46], the diameters were quite similar. Kenaf whiskers length was around 150–450 nm, with an average of 332 ± 68 nm. Based on average length and diameter measurements, the aspect ratio was 110, suggesting that cellulose kenaf whiskers have a high reinforcing capability.
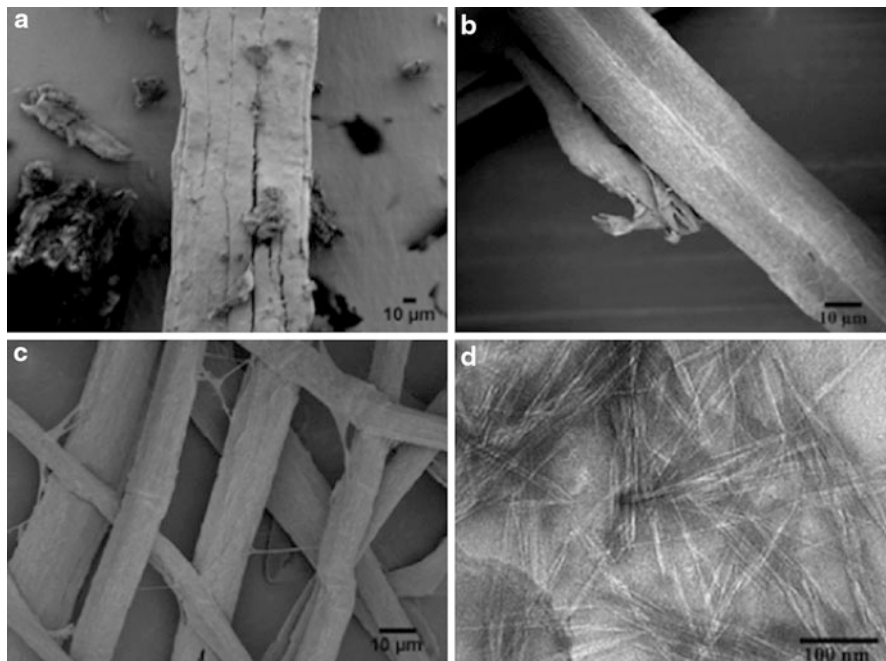
Fig. 8.4 Field emission scanning electron micrographs of (**a**) raw bast kenaf fiber and (**b**) after alkali treatment, (**c**) after alkali and bleaching, and (**d**) after alkali, bleaching, and acid hydrolysis – kenaf bast whiskers
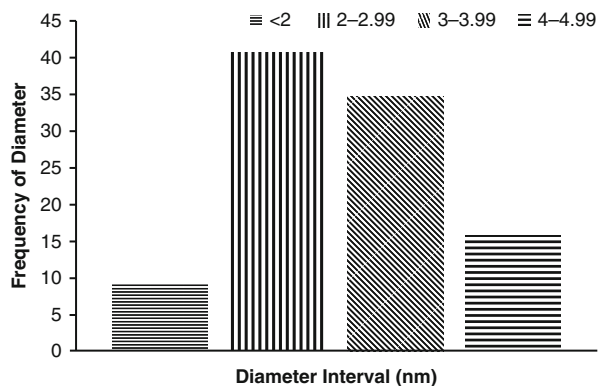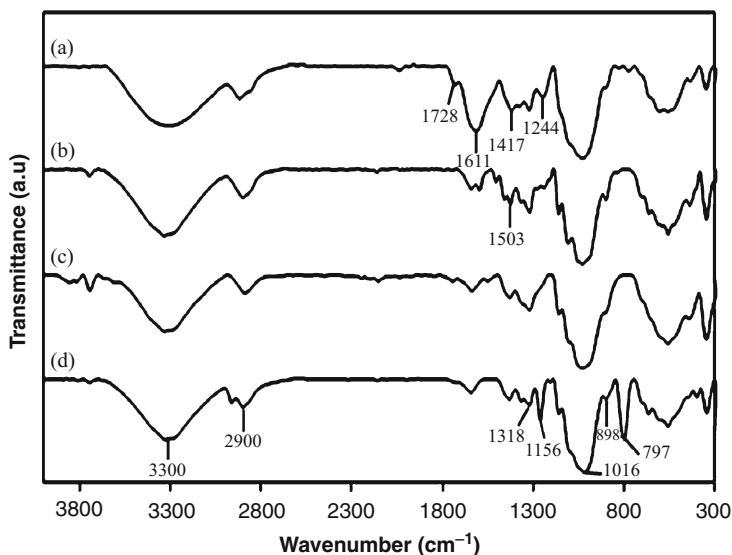

Fig. 8.5 Size distribution of kenaf bast whiskers isolated by sulfuric acid hydrolysis

3.1.3 Structural Analysis

FTIR Analysis

Infrared spectra of raw bast kenaf, alkali-treated fibers, bleached fibers, and kenaf whiskers are shown in Fig. 8.6 and summarized in Table 8.4. All spectra revealed a broad and intense peak at 3,300 cm^{-1} region which can be attributed to the

Fig. 8.6 FTIR spectra of different chemically treatment of bast kenaf fiber: (*a*) raw kenaf bast fiber, (*b*) alkali-treated fiber, (*c*) alkali-treated bleached fiber, and (*d*) kenaf whiskers

Table 8.4 FTIR characteristic peaks of kenaf bast fibers, alkali-treated fibers, bleached fibers, and kenaf whiskers samples

Kenaf bast fibers peak (cm^{-1})	Alkali-treated fibers peak (cm^{-1})	Alkali-treated bleached fibers peak (cm^{-1})	Kenaf whiskers peak (cm^{-1})	Assignment
3,324	3,335	3,332	3,329	O–H stretching
2,918	2,900	2,889	2,962	C–H symmetrical stretching and CH$_2$ symmetrical stretching
1,728	–	–	–	C = O stretching
1,612	1,642	1,637	1,641	C = C groups
1,418	1,425	1,428	1,430	C–H bonds
1,321	1,318	1,319	1,319	C–O aromatic ring
1,245	–	–	1,259	C–O stretching
–	1,158	1,156	1,157	C–O–C bond

characteristic of polysaccharides hydroxyl bonds [47]. C–H symmetrical stretching and CH$_2$ symmetrical stretching at 2,900–2,800 cm^{-1} indicated polysaccharide, wax, and oil present [47].

The peak located at 1,728 in the raw kenaf fiber was assigned to the C = O stretching of the acetyl groups of hemicelluloses and p-coumaric acids of lignin [48–50]. This peak was only seen in crude kenaf fiber suggesting the removal
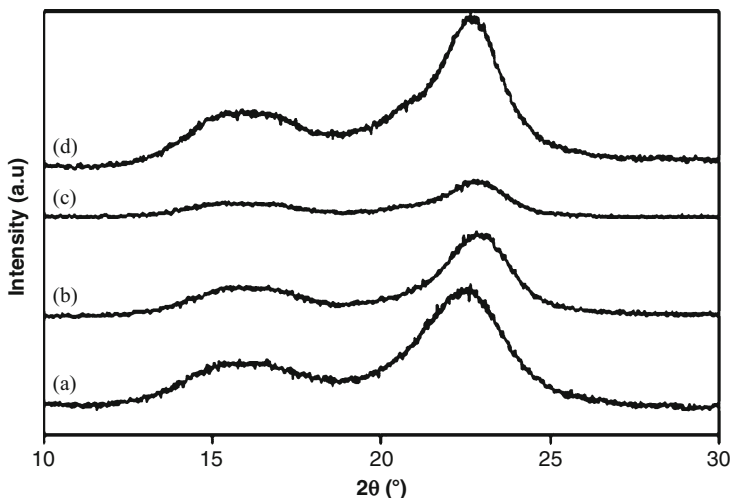
Fig. 8.7 X-ray diffraction patterns of the (*a*) raw bast kenaf, (*b*) alkali-treated fiber, (*c*) alkali-treated bleached fiber, and (*d*) kenaf whiskers

of lignin and most of the hemicellulose during the chemical treatments. The observation peak at 1,503 cm^{-1} in (b) implies that lignin was not completely removed after NaOH treatment. This peak, however, disappeared in the bleached sample (c) as well as in whiskers (d). The intensity of the peak at 1,610–1,640 corresponds to water absorbed in cellulose [47, 51]. The peak 1,430 cm^{-1} representing crystalline region in both whiskers and peak 1,417–1,427 cm^{-1} are characteristic of the C–H bonds in all organic molecules for the other samples [47, 8]. The intensity peak at 1,317–1,320 cm^{-1} region corresponds to cellulose with the C–O aromatic ring characteristic [47].

The peaks observed at 1,244 cm^{-1} in raw kenaf fiber was associated to the C–O stretching of the aryl group in lignin [47] which disappeared once the fiber was treated either with NaOH alone or bleached with aqueous chlorite. The intensity peak at 1,155–1,158 cm^{-1} region was due to the antisymmetrical deformation of the C–O–C bond [53]. The vibration peak at 898 cm^{-1} in the alkali-treated fiber and whiskers was assigned to C–H out of plane ring stretching in cellulose due to β-linkage or the glycoside bonds, which are symmetric in polysaccharides [47, 54].

X-Ray Diffraction

The X-ray diffraction of raw kenaf bast, alkali-treated fiber, alkali-treated bleached fiber, and kenaf whiskers are shown in Fig. 8.7. The crystallinity index (C$_{Ir}$) can be seen in Table 8.5. The crystallinity of the fibers increased after more treatments were applied to the fibers. Raw kenaf bast fiber had 67 % crystallinity which increased to 77 % after NaOH treatment and to 79 % after subsequent bleaching. It is believed that the removal of lignin and hemicelluloses caused the increase of its crystallinity. Kenaf whiskers generated from sulfuric acid hydrolysis only have 72 % crystallinity.

Table 8.5 Crystallinity index (C_{Ir}%) and initial degradation temperature (T_{id}) of raw, alkali-treated, alkali-treated bleached, and whiskers from kenaf bast

Material	$C_{I\%}$ (%)	T_{id} (°C)
Raw bast kenaf	67	177
Alkali-treated fibers	77	256
Alkali-treated bleached fibers	79	220
Kenaf whiskers	72	171
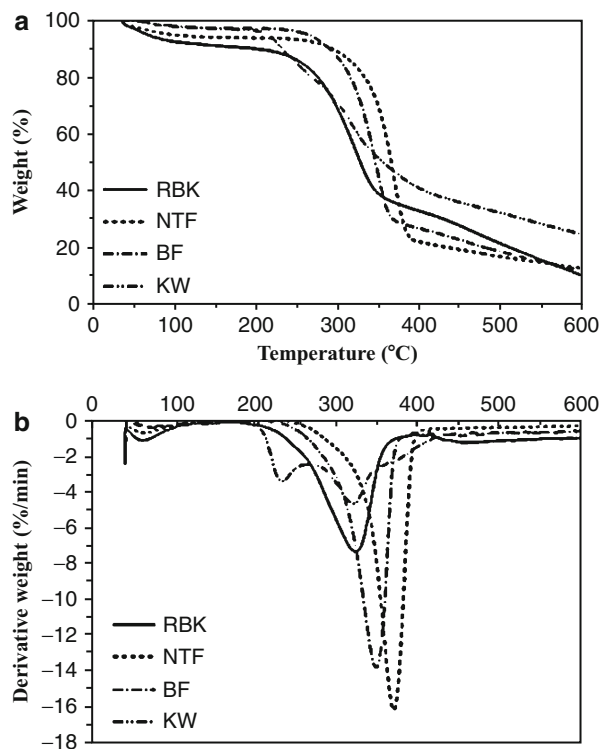
Fig. 8.8 TG and DTG curves of raw bast kenaf (*RBK*), alkali-treated fibers (*NTF*), alkali-treated bleached fibers (*BF*), and kenaf whiskers (*KW*)

Since there are many parameters that influence whiskers properties such as acid concentration, time, and temperature, the relatively lower crystallinity found in kenaf whiskers may be attributed to sulfuric acid hydrolysis reaction, attacking the crystalline region of the whiskers. Despite a lower crystallinity, kenaf whiskers formed a stable suspension which is in agreement with the study done by Araki et al. [55]. Stable suspension is an important property in order to achieve good dispersion of whiskers as matrix filler in reinforcement application.

Thermal Analysis

As reinforcement material, thermal stabilities of kenaf whiskers are important particularly in meeting minimal thermal acceptance in processing. Depending on the type of matrix/binder used, generally biocomposites are manufactured at a temperature between 150 °C and 300 °C. Figure 8.8 shows TG and DTG curves

of raw bast kenaf, alkali-treated fibers, alkali-treated bleached fibers, and kenaf whiskers. We could see from TG curves that weight loss of these samples started at 35 °C. Raw bast kenaf was observed to start degrading at 177 °C inferring degradations of both hemicellulose and lignin. Hemicellulose is very easy to remove at low temperature, while lignin degrades in a wider temperature ranging from 100 °C to 900 °C [56]. A peak at 320 °C on the DTG curve may be attributed to cellulose decomposition. The alkali-treated fibers show the greatest peak at 367 °C, while the alkali-treated bleached fibers show peak at 345 °C. Kenaf whiskers show multiple peaks at 228 °C and 316 °C that implies thermal instability, suspected to be instigated by the presence of sulfate groups on the cellulose surface. According to Wang et al. [19], thermal stability could be improved if there is less access of sulfate group onto cellulose surface. This claim may be true in the case of kenaf whiskers. The fact that kenaf whiskers recorded the lowest initial degradation temperature, i.e., 171 °C (Table 8.5), confirms its thermal instability which may be caused by the introduction of sulfate groups. The alkali-treated fibers and alkali-treated bleached fibers showed initial degradation at 256 °C and 220 °C, respectively, due to cellulose depolymerization.

3.2 Properties of Chemo-mechanical Kenaf Nanofibers

3.2.1 Chemical Composition

The chemical compositions of the kenaf fibers after various stages of chemo-mechanical treatment are presented in Table 8.6. NaOH was found to be efficient in removing the lignin from kenaf fibers. Based on the chemical composition analysis, almost all lignin was removed after bleaching process. The three-stage D1, Ep, and D2 bleaching sequence was found to increase the yield of nanofiber.

3.2.2 Fiber Morphology

The morphological structure of kenaf fibers as affected by various treatments is shown in Fig. 8.9. It was obvious that the crude kenaf fiber bundles are composed of individual fibers linked together by lignin (Fig. 8.9a). The diameter of the crude kenaf fibers ranged from 10 to 80 μm; more than 61 % of the fibers were found to have diameters between 20 and 40 μm. Figure 8.9b ,cshows structure of the fibers after pulping and bleaching processes, respectively. Clearly, both processes were able to separate the fiber bundles into individual fibers causing a significant decrease in its diameter. More than 79 % of the unbleached pulp fibers had diameters between 5 and 15 μm, and more than 88 % of the bleached pulp fibers displayed diameters between 1 and 8 μm. Figure 8.9d, e depicts the morphology of the unbleached and bleached pulp fibers after the refining process and cryo-crushing, respectively. The image analysis study showed that 49 % of the unbleached pulp fibers as well as 58 % of the bleached pulp fibers have diameters 0.1–1 μm. These results proved that the diameter of kenaf fiber can be reduced to nanosize by applying PFI refining followed by cryo-crushing.

Table 8.6 Chemical compositions of kenaf stem, bast, and core fibers after being subjected to different treatments

Materials		Cellulose (%)	Hemicellulose (%)	Lignin (%)	Extractive free (%)	Ash (%)
NaOH-treated fibers	Stem	58.00 ± 1.0	22.0 ± 1.0	17.50 ± 1.3	1.70 ± 0.2	2.40 ± 0.4
	Bast	81.5 ± 1.0	12.7 ± 1.9	2.5 ± 0.3	0.9 ± 0.4	2.2 ± 0.8
	Core	46.0 ± 0.5	33.0 ± 2.0	20.0 ± 1.0	2.20 ± 0.5	3.0 ± 0.4
Bleached pulp	Stem	91.00 ± 1.0	6.00 ± 1.8	1.00 ± 00	1.00 ± 0.5	0.25 ± 00
	Bast	92.0 ± 1.4	5.2 ± 0.6	0.5 ± 0.4	0.5 ± 0.3	–
	Core	92.0 ± 1.0	4.00 ± 1.0	0.70 ± 0.6	1.50 ± 0.2	0.5 ± 0.5
Bleached nanofibers	Stem	92.00 ± 0.5	5.00 ± 0.7	0.50 ± 0.5	0.60 ± 0.3	0.20 ± 00
	Bast	92.8 ± 0.5	46.0 ± 0.5	0.5 ± 0.3	0.4 ± 0.1	–
	Core	94.0 ± 0.5	4.7 ± 0.7	0.50 ± 0.5	0.80 ± 0.5	0.5 ± 0.1

The transformation of kenaf fibers from crude to nanosize is depicted in Fig. 8.10a–c. Clearly, the surface of the raw fiber (scale in 50 μm) was covered by a number of impurities suspected to be hemicellulose, lignin, pectin, and waxy substances. Conversely, the surface of bleached pulp fibers (scale in 50 μm) was much cleaner and smoother. Pulping had seemingly extracted out almost all hemicellulose and some lignin, while the subsequent bleaching practically removed all the lignin. Figure 8.10c demonstrates TEM image of kenaf nanofibers (scale in 1 μm) generated in this study which noticeably fall within nanosize (<100 nm).

3.2.3 Structural Analysis

FTIR Analysis

The IR spectra of the kenaf fibers after different treatments are shown in Fig. 8.11 [57]. The absorbance peaks in the 3,400–3,300 cm^{-1} region were attributed to the stretching of O–H groups, whereas those around 2,900–2,800 cm^{-1} were due to the stretching of C–H [58]. The peak located at 1,731 cm^{-1} in the raw kenaf was assigned to the C = O stretching of the acetyl group in hemicellulose [64, 65] or the ester linkage of carboxylic group in the ferulic and p-coumeric acids of lignin and/or hemicellulose [59]. This peak disappeared completely in the spectra of the unbleached and bleached pulps as well as for the bleached and unbleached nanofibers, thus indicating the removal of lignin and hemicellulose after these processes. In the raw kenaf, the peak at 1,242 cm^{-1} was associated to the C–O stretching of the aryl group in lignin [47]. Detailed explanation of absorbance peaks has been reported by Mehdi et al. [57].

X-Ray Diffraction

The X-ray diffractograms and crystallinity indices of the unbleached fibers, bleached pulp fibers, and nanofibers are shown in Fig. 8.12 and Table 8.7.
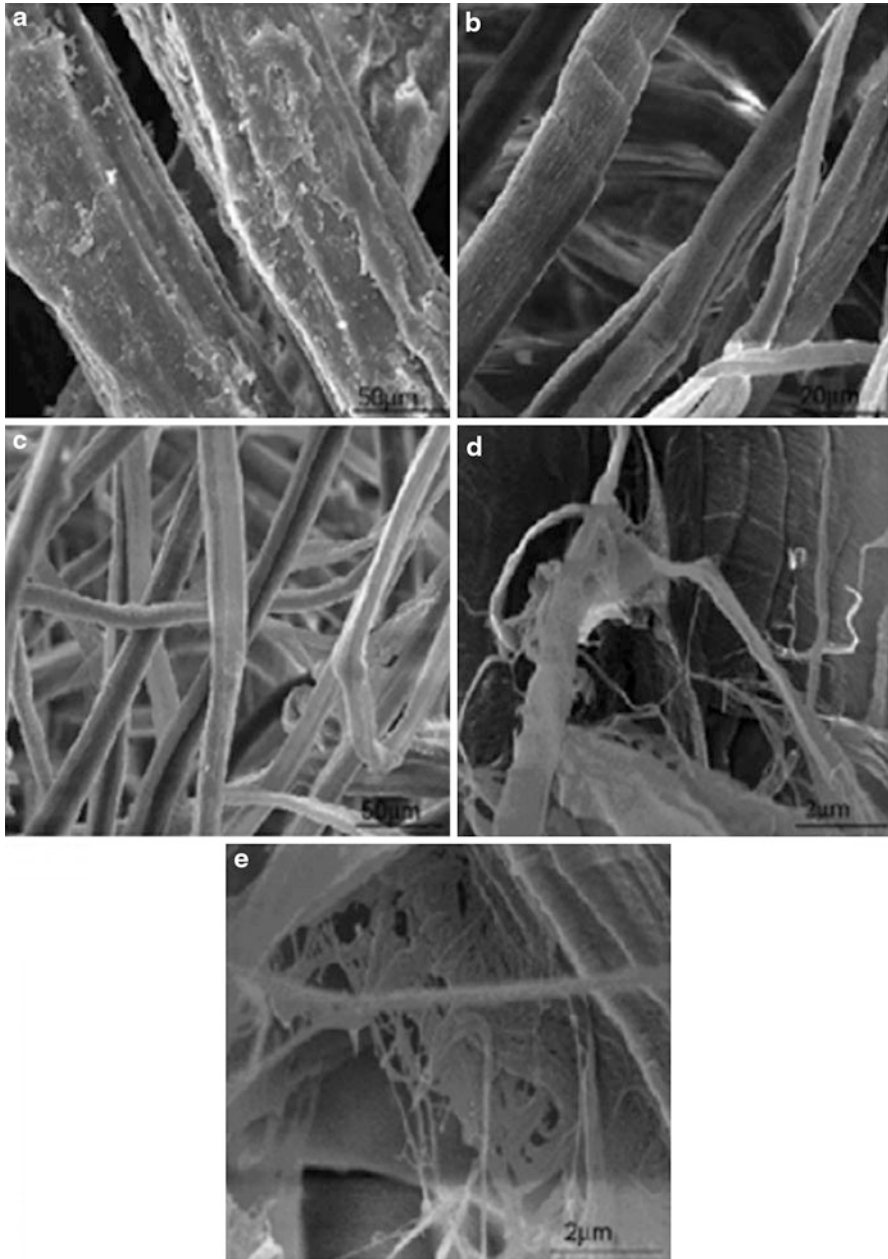
Fig. 8.9 ESEM micrographs of the structure of the kenaf fibers before and after chemical treatment for (**a**) raw kenaf fibers, (**b**) unbleached pulp, (**c**) bleached pulp, (**d**) fibers after cryo-crushing and treatment in a PFI mill, and (**e**) bleached pulp after cryo-crushing and treatment in a PFI mill [57]
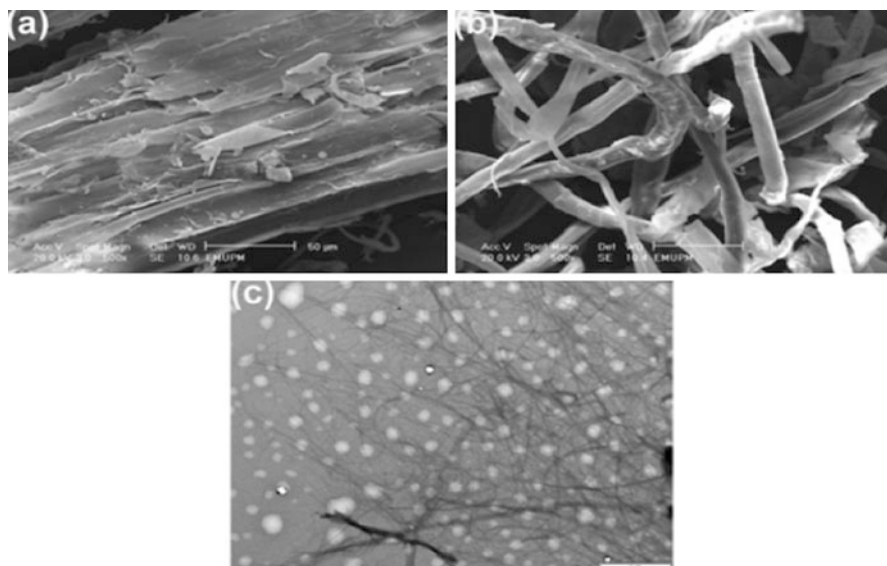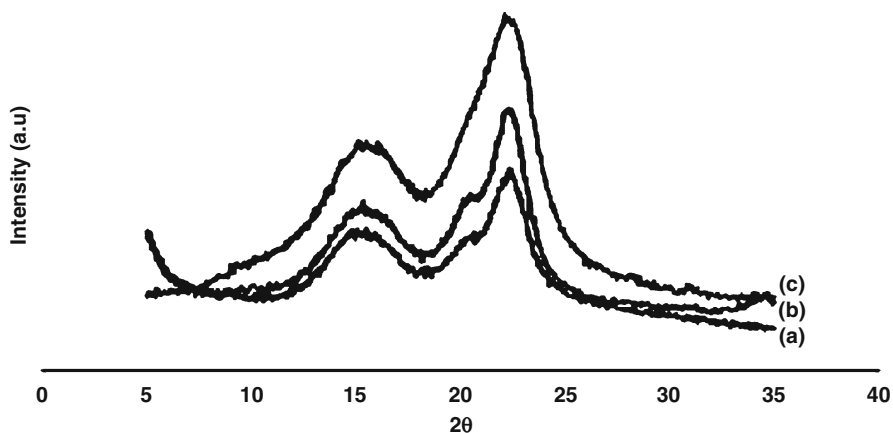
Fig. 8.10 Micrographs of (**a**) raw fibers, (**b**) bleached pulp fibers (chemo-mechanical treatments), and (**c**) TEM image of kenaf nanofibers
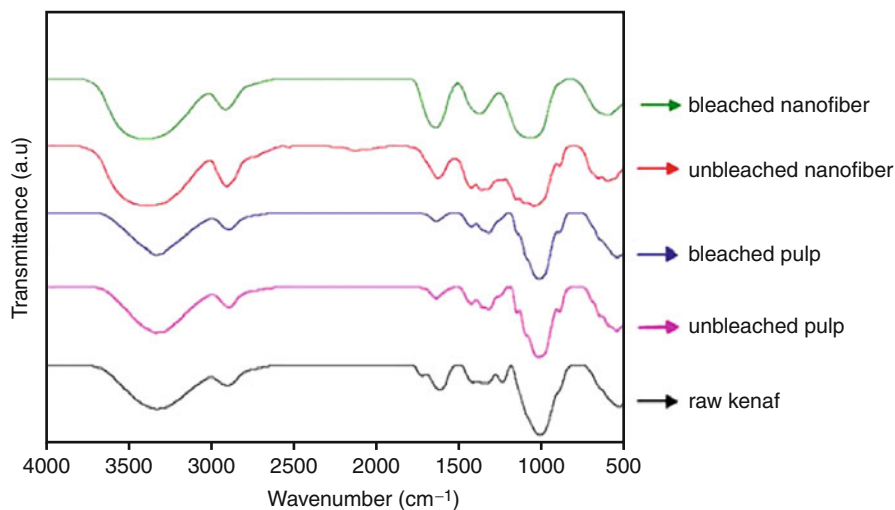
Fig. 8.11 Infrared spectra of kenaf fibers after various treatment

The crystallinity pattern of native cellulose (cellulose I) was exhibited by all of the samples. However, in contrast with the fibers, there were no crystalline transformations in the structures of the treated samples which displayed their major peak intensities at 2θ values close to $22.5°$.

Fig. 8.12 X-ray diffraction patterns of (*a*) raw fibers, (*b*) bleached pulp fibers, and (*c*) nanofibers

Table 8.7 The crystallinity of the kenaf stem, bast, and core fibers before and after chemo-mechanical treatments

Material		Crystallinity (%)
Fibers	Stem	44
	Bast	68
	Core	41
Bleached pulp	Stem	60
	Bast	77
	Core	53
Bleached nanofibers	Stem	67
	Bast	81
	Core	62

These results clearly demonstrate the increase in the degree of crystallinity after chemo-mechanical treatments. The results also pointed towards the large difference in crystallinity between the raw kenaf fiber (41–68 %) and the bleached nanofiber (62–81 %). Among the kenaf types, the bast has the highest crystallinity at all levels of treatment. According to Alemdar and Sain [59], the increase in crystallinity is caused by greater removal of lignin and hemicellulose. The results gathered from the X-ray diffraction measurements also demonstrated that the mechanical treatments had some effects on the degree of crystallinity of the cellulose fiber. In this case, the proportion of crystalline regions was increased significantly after being subjected to high-pressure homogenization. On the other hand, cellulose nanofibers comprise pure cellulose chains, causing the crystallinity index to be higher. It is believed that higher crystallinity leads to higher tensile strength of the fiber and thereby may improve mechanical properties of the corresponding nanocomposites [59].

Thermogravimetric Analysis (TGA)

The thermal behavior of lignocellulosic materials depends on their chemical composition, structure, and degree of crystallinity [60]. In the case of kenaf bast fibers, the raw fiber cellulose decomposition occurred at 306 °C, while the bleached pulp and nanofibers were at 330 °C and 341 °C, respectively. The degradation temperatures for raw kenaf, unbleached pulp, bleached pulp, unbleached nanofibers, and bleached nanofibers were at 313 °C, 321 °C, 342 °C, 348 °C, and 351 °C, respectively.

The higher amount of residue in the raw kenaf fiber as opposed by the fibers after chemo-mechanical treatments was due to the presence of ash as well as lignin, which have a very slow degradation [56, 61].

4   Conclusions

Cellulose nano fibers can be produced from kenaf whole stem, bast, and core. Isolation of kenaf whiskers from raw bast kenaf via sulfuric acid hydrolysis was successfully conducted without apparent degradation of the cellulose. Treating the fiber with NaOH followed by bleaching in aqueous chlorite is effective in removing lignin and hemicellulose in the fiber. The kenaf whiskers produced in this study had crystallinity of 71 % and was able to form a stable suspension.

Cellulose nanofibers can also be isolated from kenaf stem via chemo-mechanical extraction. The nanofibers isolated from kenaf stem fibers had diameters 15–25 nm, whereas kenaf core, 20–25 nm. Chemical analysis of the fiber after each stage of treatment exhibited an increase in cellulose content and a decrease in lignin and hemicellulose content. The results from the FTIR confirmed that the lignin, as well as most of hemicellulose, can be removed during the chemical process. The TGA analysis demonstrated that the thermal stability of fibers improved after chemo-mechanical treatments. The crystallinity results showed that the chemo-mechanical treatments are more effective in increasing the crystalline structure of the kenaf cellulose. Among the kenaf sections, nanofiber produced from bast has the highest crystallinity (81 %). Both kenaf whiskers and nanofibers formed a stable suspension.

References

1. Rousseau S, Tolnai B (2010) Method of manufacturing nano-crystalline cellulose film. US 2010/0124651 A1
2. Christiane L (2012) Hemicellulose and cellulose modifications. In: Sundqvist H (ed) Research highlights in industrial biomaterials, vol 2. VTT Research Highlights, Espool, pp 31–46

3. Xanthos M (2005) Chapter 2, Modification of polymer mechanical and rheological properties with functional fillers. In: Xanthos M (ed) Functional fillers for plastics. Wiley-VCH, Weinheim, FRG, p 21
4. Samir MASA, Alloin F, Defresne A (2005) Review of Recent Research into Cellulosic Whiskers, Their Properties and Their Application in Nanocomposite Field. Biomacromolecules 5:612–626
5. Koo JH (2007) What are nanoplastics? The Future of Nanoplastics, 22–23 Feb 2007, San Antonio
6. Simonsen J (2005) Bio-based nanocomposites: challenges and opportunities. In: Society of Wood Science and Technology 48th annual convention, 19 June 2005, Quebec, Canada
7. Winandy JE, Rudie AW, Williams RS, Wegner TH (2008) Integrated biomass technologies: future vision for optimally using wood and biomass. For Prod J 58(6):6–16
8. Berglund L, Mohanty AK, Misra M, Drzal L (2005) Natural Fibers, Biopolymers, and Biocomposites. CRC Press, Boca Raton, pp 807–832
9. Wågberg L, GeroDecher MN, Tom Lindström MA, Karl A (2008) Cellulose-based nanocomposites. Langmuir 24(3):784–795
10. Tatsumi D, Satoshi I, Takayoshi M (2002) Effect of Fiber Concentration and Axial Ratio on the Rheological Properties of Cellulose Fiber Suspensions. J Soc Rheol 30(1):27–32
11. Pääkkö M, Ankerfors M, Kosonen H, Nykänen A, Ahola S, Österberg M, Ruokolainen J, Laine J, Larsson PT, Ikkala O, Lindström T (2007) Enzymatic Hydrolysis Combined with Mechanical Shearing and High-Pressure Homogenization for Nanoscale Cellulose Fibrils and Strong Gels. Biomacromolecules 8(6):1934–1941
12. Tahir PM, Amel BA, Syeed OA, Saiful A, Zakiah A (2011) Retting Process Of Some Bast Plant Fibres And Its Effect On Fibre Quality: A Review. BioResources 10(4):1–8
13. Wood I (2000) Fibre crops-new opportunities for Australian agriculture. CSIRO, Brisbane
14. Rymsza TA (2000) Advancements of kenaf in the USA-kenaf paper and nonpaper developments. In: International kenaf conference, Japan Kenaf Association, p 10
15. Kozlowski R (2000) Potential and diversified uses of green fibers. In: 3rd international wood and natural fibers, composites symposium, pp 1–14
16. Fisher G (1994) Proceeding of the Tappi pulping conference 1994. Tappi Press, Atlanta, pp 91–94
17. FAO (2006) Jute, kenaf, sisal, aabaca, coir and allied fibers statistics. http://www.fao.org/es/esc/en/20953/21005/highlight_51023en
18. Liu W, Drzal LT, Mohanty AK, Misra M (2007) Influence of processing methods and fiber length on physical properties of kenaf fiber reinforced soy based biocomposites. Compos B 38(3):352–359
19. Wang B, Sain M, Oksman K (2007) Study of Structural Morphology of Hemp Fiber from the Micro to the Nanoscale. Appl Compos Mater 14(2):89–103
20. Amel BA, Paridah MT, Sudin R, Anwar U, Hussein AS (2013) Effect of fiber extraction methods on some properties of kenaf bast fiber. Industrial Crops and Products 46:117–123
21. Rowell RM, Stout HP (1998) Jute and kenaf. In: Handbook of fiber chemistry, 2nd edn. Marcel Dekker, New York, pp 465–504
22. Zhang T (2003) Improvement of kenaf yarn for apparel applications. Master thesis of Louisiana State University
23. Rowell RM, Han JS (2000) Characterisation and factors effecting fiber properties. In: Frolini E, Leao AL, Mattosso LHC (eds) Natural polymers and agrofibers composites. Embrapa Instrumentacao Agropecuaria, San Carlos, pp 115–127
24. Chen L, Columbus EP, Pote JW, Fuller MJ, Black JG (1995) Kenaf bast and core separation. Kenaf Association, Irving, pp 15–19
25. Calamari TA, Tao W, Goynes WR (1997) A preliminary study of kenaf fiber bundles and their composite cells. Tappi J 80(8):149–154
26. Abdul Khalil HPS, Ireana Yusra AF, Bhat AH, Jawaid M (2010) Cell wall ultrastructure, anatomy, lignin distribution, and chemical composition of Malaysian cultivated kenaf fiber. Indus Crops Prod 31(1):113–121

27. Voulgaridis E, Passialis C, Grigoriou A (2000) Anatomical characteristics and properties of kenaf stems (Hibiscus cannabinus). IAWA J 21(4):435–442
28. Calamari TA, Tao W, Andrew ED (1999) Kenaf properties, processing and products. Mississippi State University, Mississippi, pp 32–57
29. Misra DK 1987. Cereal Straw: Chapter VI in Pulp and Paper Manufacture; Secondary Fibers and Non-Wood Fibers. In: Hamilton F, Leopold B (eds). TAPPI, Atlanta, GA
30. Mohanty AK, Misra M, Drzal LT (2001) Surface modifications of natural fibers and performance of the resulting biocomposites: an overview. Compos Interfaces 8(5):313–343
31. Anon (2001) Kenaf – an alternative fiber crop. Natural Life Magazine, International Kenaf Association, p 42
32. Sikorski J (1963) The fine structure of animal and man-made fibers. In: Hearle JWS, Peters RH (eds) Fiber structure. Butterworth & Company/The Textile Institute, London, pp 269–310
33. Mwaikambo LY, Ansell MP (2005) Mechanical properties of alkali treated plant fibers and their potential as reinforcement materials. Part I. Hemp fiber, Journal of Materials Science, 41(8): 2483–2496
34. Preston RD (1963) Observed structure in plant fibers. In: Hearle JWS, Peters RH (eds) Fiber structure. Butterworth & Company/The Textile Institute, London, pp 235–268
35. Ranalli P (1999) Advances in hemp research. Haworth Press: Binghamton, NY, p 272
36. Mwaikambo LY (2002) Plant-based resources for sustainable composites. PhD thesis, University of Bath, Department of Engineering and Applied Science, Bath
37. Alemdar A, Sain M (2008) Biocomposites from wheat straw nanofibers: morphology, thermal and mechanical properties. Compos Sci Technol 68(2):557–565
38. Wang B, Sain M (2007) Dispersion of soybean stock-based nanofiber in a plastic matrix. Polym Int 56(4):538–546
39. Taniguchi T, Okamura K (1998) New films produced from microfibrillated natural fibres. Polym Int 47(3):291–294
40. Chakraborty A, Sain M, Kortschot M (2005) Cellulose microfibrils: a novel method of preparation using high shear refining and cryocrushing. Holzforschung 59(1):102–107
41. Nakagaito AN, Yano H (2005) Novel high-strength biocomposites based on microfibrillated cellulose having nano-order-unit web-like network structure. Appl Phys A 80(1):155–159
42. Oksman K, Sain M (2006) Introduction to cellulose nanocomposites. In: Cellulose nanocomposites; processing, characterization and properties, ASC symposium series 938, Oxford Press, pp 2–8
43. Bhatnagar A., Sain M (2003) Manufacturing of nanofibrils. Canadian Patent 02437616
44. Wise LE, Murphy M (1946) Chlorite Holocellulose, its Fractionnation and Bearing on Summative Wood Analysis and on Studies on the Hemicelluloses. Pap Trade J 122:35–43
45. Brigham JS, Adney WS, Himmel ME (1996) Handbook on bioethanol: production and utilization. Taylor and Francis, Washington, DC, pp 119–141
46. Teixeira SR, Agda Eunice de Souza, Angel Fidel Vilche Peña, Regiane Godoy de Lima, Álvaro Gil Miguel (2011) Use of charcoal and partially pirolysed biomaterial in fly ash to produce briquettes: sugarcane bagasse, alternative fuel. Maximino Manzanera (ed)
47. Troedec M, Sedan D, Peyratout C, Bonnet J, Smith A, Guinebretiere R, Gloaguen V, Krausz P (2008) Influence of various chemical treatments on the composition and structure of hemp fibres. Compos A 39(3):514–522
48. Biogiotti J, Puglia D, Kenny JM (2004) A review on natural fibre-based composites-part I: structure, processing and properties of vegetable fibres. J Nat Fib 1(2):37–68
49. Liu W, Mohanty AK, Drazal LT, Askel P, Misra M (2004) Effects of alkali treatment on the structure, morphology and thermal properties of native grass fibers as reinforcements for polymer matrix composites. J Mater Sci 39(3):1051–1054
50. Sun XF, Xu F, Sun RC, Fowler P, Baird MS (2005) Characteristics of degraded cellulose obtained from steam-exploded wheat straw. Carbohydr Res 340(1):97–106

51. Nacos M, Katapodis P, Pappas C, Daferera D, Tarantilis PA, Christakopoulos P, Polissiou M (2006) Kenaf xylan - A source of biologically active acidic oligosaccharides. Carbohydr Polym 66(1):126–134

52. Keshk S, Suwinarti W, Sameshima K (2006) Physicochemical characterization of different treatment sequences on kenaf bast fiber. Carbohydr Polym 65(2):202–206

53. Silva MC, Lopes OR, Colodette JL, Porto AO, Rieumont J, Chaussy D, Belgacem MN, Silva GG (2008) Characterization of three non-product materials from a bleached eucalyptus kraft pulp mill, in view of valorising them as a source of cellulose fibres. Ind Crop Prod 27(3):288–295

54. Adel AM, Abd El-Wahab ZH, Ibrahim AA, Al-Shemy MT (2011) Part II: physicochemical properties. Carbohydr Polym 83(2):676–687

55. Araki J, Wada M, Kuga S, Okano T (2000) Flow properties of microcrystalline cellulose suspension prepared by acid treatment of native cellulose. Colloids Surf A Physicochem Eng Asp 142(1):75–82

56. Yang H, Yan R, Chen H, Lee D, Zheng C (2007) Characteristics of hemicellulose, cellulose and lignin pyrolysis. Fuel 86:1781–1788

57. Mehdi J, Jalaludin H, Alireza S, Manjusri M, Kristiina O (2009) Chemical composition, crystallinity, and thermal degradation of bleached and unbleached kenaf bast (Hibiscus cannabinus) pulp and nanofibers. BioResources 4(2):626–639

58. Khalil HPA, Ismail H, Rozman HD, Ahmad MN (2001) The effect of acetylation on interfacial shear strength between plant fibres and various matrices. Eur Polym J 37(5):1037–1045

59. Alemdar A, Sain M (2007) Isolation and characterization of nanofibers from agricultural residues–Wheat straw and soy hulls. Bioresour Technol 99(6):1664–1671

60. Fisher T, Hajaligol M, Waymack B, Kellogg D (2002) Pyrolysis behavior and kinetics of biomass derived materials. J Anal Appl Pyrol 2(2):331–349

61. Ashori A, Jalaluddin H, Raverty WD, MohdNor MY (2006) Chemical and morphological characteristics of Malaysian cultivated kenaf (Hibiscus cannabinus) fiber. Polym-Plast Technol Eng J 45(1):131–134

62. Clemons CM, Canlfieid DF (2005) Natural fibers, Chapter 11. In: Xanthos M (ed) Functional fillers for plastics. Wiley-VCH, Weinheim

63. Siqueira G, Abdillahi H, Bras J, Dufresne A (2010) High reinforcing capability cellulose nanocrystals extracted from Syngonanthus nitens (Capim Dourado). Cellulose 17(2):289–298

64. Sgriccia N, Hawley M, Misra M (2008) Characterization of natural fiber surfaces and natural fibre composites. Compos. Part A-Appl. S. 39(10):1632–1637

65. Tserki V, Zafeiropoulos NE, Simon F, Panayiotou C (2005) A study of the effect of acetylation and propionylation surface treatments on natural fibres. Composites Part A 36:1110–1118

66. Gassan J, Chate A, Bledzki AK (2001) Calculation of elastic properties of natural fibres. J. Mater. Sci. 36(15): 3715–3720

67. Alann A (2006) Fibres for strengthening of timber structures. Research report: 03, http://www.google.com.my/#hl=en&&sa=X&ei=F1bATP6sOZL5cZqslJoM&ved=0CBQQvgUoAA&q, Accessed on 21.10.2010

68. Rowell RM, Sanadi AR, Caulfield DF, Jacobson RE (1997) Utilization of natural fibers in plastic composites: problems and opportunities. Lignocellulosic-plastic composites: 23–51